Thermotropism in Tail-End (Dimethylamino)pyridinium Polymethacrylates with Bromine and Octylsulfonate Counterions

Pascal Y. Vuillaume,[‡,§] Xavier Sallenave,[†] and C. Geraldine Bazuin*[,†,‡]

Département de chimie, Université de Montréal, C.P. 6128 Succ. Centre-Ville, Montréal (QC), Canada H3C 3J7, and Département de chimie, Université Laval, Cité universitaire, Québec (QC), Canada G1K 7P4

Received June 30, 2006; Revised Manuscript Received September 20, 2006

ABSTRACT: Polyamphiphiles of the type poly(ω-dimethylaminopyridinium bromide alkyl methacrylate)s with octyl, dodecyl, and hexadecyl spacers were synthesized and further self-assembled with octylsulfonate to form stoichiometric complexes. The thermal and structural properties of both the bromine- and octylsulfonate-neutralized series (PnDMAP-Br and PnDMAP-S8, $n = 8$, 12, 16) were investigated in the bulk. For $n = 8$ in both series and $n = 12$ in the Br series, the materials are essentially amorphous with weak mesomorphic order. For $n = 12$ in the S8 series and $n = 16$ in both series, crystalline and disordered lamellar (smectic A) structural order is observed. Recrystallization is slow after melting, especially for P16DMAP-S8, which can be maintained indefinitely in its liquid crystal state even well above room temperature. This is attributed to the ionic interactions coupled with the polymeric character of the materials as well as, possibly, surfactant chain and polyamphiphile spacer interactions in the complexes. The liquid crystal−isotropic transition (observed clearly by DSC for $n = 16$ in both series, but not for P12DMAP-S8) is also affected. Plasticization by the spacer and surfactant tail reduces the well-defined glass transitions (T_g's) of the materials, but this is mitigated by the presence of the ionic groups (the lowest T_g measured, for P16DMAP-S8, is near room temperature). The lamellar period depends on the spacer length but hardly on the counterion. The properties of the two series are compared with those of other tail-end polyamphiphiles and complexes to offer an overall perspective on the bulk behavior of this class of materials, some of which are ideal candidates for forming anisotropic glasses.

Introduction

Ion-containing polyamphiphiles (iPA's) covalently link hydrophobic fragments and ionic groups within the same macromolecular chain. iPA's are ideally suited for self-assembly and are, for example, good candidates for participating in structure formation in organic−inorganic multilayer thin films.[1,2] iPA's may be designed with various types of geometry;[3] of these, the tail-end type, i.e., where the ionic groups are attached at the end of hydrophobic side chains, is reminiscent of the classic side-chain liquid crystal polymer geometry. In contrast to the latter, there are only a few studies of the thermal and structural behavior of tail-end iPA's in the bulk, and a limited number of structure−property relationships have been established. Since the presence of ionic groups strongly influences many material properties, including those of thermotropic materials,[4,5] it is important to investigate these relationships in view of various applications.

We have previously described the synthesis and bulk properties and structure of a series of poly(ω-substituted pyridinium bromide alkyl methacrylates), mainly with a dodecyl spacer.[6] These materials tend to self-organize into a disordered smectic-like phase whose detailed characteristics (lamellar thickness, correlation length) depend on the spacer length and on the chemical nature of the pyridinium group. Their glass transition temperatures are high (above ambient) compared to analogous nonionic side-chain polymers and, in conjunction with a rigid, elongated pyridinium moiety, can be as high as that of poly(methyl methacrylate) despite the long flexible spacer. They may thus be useful as anisotropic glasses. Like for other tail-end polyamphiphiles studied,[7−10] they typically show no well-defined thermotropic transition or crystallinity, not even for a long, 16-methylene spacer (investigated for a methylpyridinium tail-end moiety, MP). On the other hand, when the Br^- counterions are exchanged for long alkyl (hexadecyl) sulfonate counterions (again, investigated with the MP polyamphiphile), thermotropic materials with semicrystalline and smectic A-like phases can be obtained; shorter surfactants (*n*-butyl- and *n*-octylsulfonates) were not observed to induce this behavior.[11] In the case of the pyridylpyridinium (PP) bromide dodecyl methacrylate polyamphiphile, addition of a (relatively short) hydrogen-bonding surfactant, octylphenol, also leads to the formation of a thermotropic liquid crystalline material with a semicrystalline and a smectic A phase.[12]

In the present work, we extend the above studies to examine the impact of the variation of the spacer length (8, 12, and 16 methylene units) in conjunction with bromine vs octylsulfonate counterions on the thermotropic behavior of a methacrylate polyamphiphile with a relatively bulky pyridinium end group, namely (4-dimethylamino)pyridinium (DMAP) (Figure 1). This polyamphiphile was earlier found to be the least organized of the pyridinium polyamphiphiles with a 12-methylene spacer and bromine counterion.[6] It is also noteworthy that there may be charge delocalization over the DMAP moiety,[13] which may have some impact on the localization of the counterion. The behavior of this series of polyamphiphiles will be compared with the previously studied series to offer an overall perspective on the bulk behavior of this class of materials. It may be added that another motivation for studying the present series is related to their potential as gene delivery vectors.[14]

* To whom correspondence should be addressed. Current address: Université de Montréal. E-mail: geraldine.bazuin@umontreal.ca.
† Université de Montréal.
‡ Université Laval.
§ Current address: Faculté de médecine vétérinaire et Institut de biotechnologie vétérinaire et alimentaire, Université de Montréal, 3200 rue Sicotte, St-Hyacinthe (QC), Canada J2S 2M2.

10.1021/ma061477j CCC: $33.50
Published on Web 11/07/2006

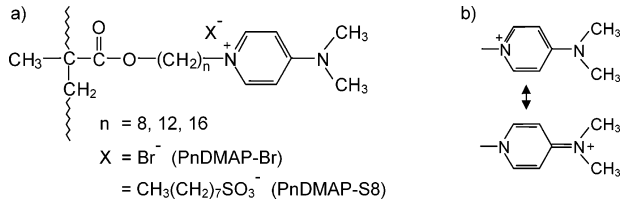

Figure 1. (a) Chemical structure of the polyamphiphiles (PnDMAP-Br) and polyamphiphile−surfactant complexes (PnDMAP-S8) studied. (b) Possible resonance structures of the DMAP moiety.

Experimental Section

Materials. The reagents for polymerization are specified in ref 6. Sodium octylsulfonate (S8-Na, 98%) and 2-mercaptoethanol (ME), from Aldrich, were used as received. Dialysis membranes (SpectraPor, VWR) had a nominal cutoff of 6000−8000 Da (3500 for $n = 8$). All solvents used were of analytical grade. Water used for polymerization and dialysis was purified by a Milli-Q water purification system (resistance 18.2 MΩ).

Techniques of Analysis. Elemental analysis reported for the elements C, H, N, O, S, and Br was conducted at Institut Charles Sadron (Strasbourg, France), whereas that restricted to the elements C, H, N, and S was done at Université de Montréal. NMR spectra were recorded using Bruker 300 and 400 MHz spectrometers; chemical shifts, δ, are given in ppm relative to the solvent residual resonances fixed at 4.61 (4.31 at 70 °C[15]), 7.27, and 2.49 ppm for D_2O, $CDCl_3$, and $CD_3(SO)_2$, respectively. To monitor the presence or absence of Na and Br ions in the polyamphiphile/surfactant complexes, energy-dispersive X-ray microanalysis (EDX) was performed on samples coated with Au/Pd alloy, using a JEOL JSM-840A and Hitachi S-3000N scanning electron microscope system.

Thermogravimetric analysis (TGA) was effected using a Mettler TA 3000 TGA, operated under constant nitrogen flow (200 mL/min) and a heating rate of 5 °C/min. The samples were previously dried in vacuo at 60 °C and then in situ at 80 °C for 10 min just prior to the heating scans. The temperature of thermal degradation is reported as the point of 5% weight loss relative to the weight at 80 °C.

Differential scanning calorimetry (DSC) was carried out using a Perkin-Elmer DSC-7 calorimeter calibrated with In and flushed with He. The complexes were placed in aluminum pans with pierced covers and dried in vacuo at about 100 °C for at least 2 days (unless otherwise specified). The surfactant was previously dried at 90 °C in vacuo overnight. Unless otherwise noted, scans were recorded at 20 °C/min. Except for first heating and unless otherwise noted (see Results and Discussion), the scans are reproducible. Glass transition temperatures (T_g) are given as the midpoint of the heat capacity jump, and first-order transition temperatures are given by the peak maximum or minimum and correspond to average values for at least two samples and three scans.

Polarizing optical microscopy (POM) observations of the samples were made using a Zeiss Axioskop microscope equipped with a 25× Leica objective, a Mettler FP5 temperature controller, and a FP52 hot stage.

X-ray diffractometry (XRD) was carried out using Rigaku and Bruker diffractometers. In the Rigaku apparatus, nickel-filtered Cu Kα radiation ($\lambda = 1.542$ nm) was produced by a rotating anode X-ray generator (Rotaflex RU-200BH) operated at 55 kV and 190 mA, and collimation was effected by a Soller slit and a 1 mm pinhole. The diffraction profiles, for 2θ angles varying between 1.1° and 30°, were scanned by a Rigaku scintillation counter (SC-30) coupled to a pulse-height analyzer. Temperature was controlled by a homemade water-cooled copper block oven. In the Bruker apparati, the X-ray beam was generated by the Kristalloflex K760 or K760-80 generator from a sealed tube Cu anode, and collimation was effected using a graphite monochromator and a 0.5 mm pinhole collimator. The diffraction pattern was recorded by a Bruker AXS two-dimensional position-sensitive wire-grid detector, and that for an empty capillary was subtracted from the integrated profiles (except those shown in Figure 6). Temperature was regulated initially by a Watlow 988 controller and oven supplied by Bruker and later by an Instec HCS400/410 hot and cold stage with a STC 200 controller. The samples were placed in 1.0 or 1.5 mm i.d. Lindemann capillaries (Charles Supper), dried in vacuo at 60 °C for 4 days followed by 2 days at 100 °C (unless otherwise specified), and then sealed.

The d spacings were determined from the diffraction peaks using Bragg's relation, $d = \lambda/(2 \sin \theta)$. Calculated molecular lengths (l_c) were estimated using Hyperchem (Hypercube Inc.) for the lowest energy conformation of the side chain or surfactant with all-trans methylene units, including van der Waals radii at the extremities. For the polymer, this length corresponds to the distance from the outermost hydrogen of the methyl group on the polymer backbone to the terminal atom of the side chain.

Synthesis. The synthesis of P12DMAP-Br, involving free radical polymerization in aqueous micellar solution, is described elsewhere.[6] P8DMAP-Br was synthesized in the same conditions. P16DMAP-Br and a second batch of P12DMAP-Br were also synthesized following the published procedure, except that polymerization was carried out in the presence of a small amount of transfer agent, 2-mercaptoethanol (ME), to reduce the molar mass in view of improving polymer solubility.[11] The molar ratio of ME to monomer was 0.06; the monomer concentration was 0.2 mol/L, and the initiator (4,4′-azobiscyanovaleric acid, sodium salt) to monomer molar ratio was 0.01. The polymers were purified by dialysis in water for 3 days, and the absence of unreacted monomer was verified by ^{1}H NMR. The two batches of P12DMAP, polymerized without and with ME, will be referred to hereafter as P12DMAP*a* and P12DMAP*b*, respectively (the latter was used entirely for ion-exchanging with S8). Reliable molecular weights of these polyamphiphiles are difficult to determine.[6,11] However, based on the absence of any NMR signal due to initiator end-group moieties (a CH_2 signal from ACVA is expected between 1.8 and 2.3 ppm, a region free of any signal from the complex, as tested in DMSO-*d* for both P12DMAP-S8 complexes and for ACVA using a 400 MHz NMR), the molecular weight appears to be well over 10 000, noting that a study with an analogous polyamphiphile (PP) indicates that the T_g is constant for molecular weights starting at about 10 000 (as determined by osmometry).[12,16]

Preparation of Complexes. Complexes were prepared by the procedure described previously.[11] Briefly, the dialysis bag containing the purified Br-neutralized polymer (left in its aqueous solution) was placed in an aqueous solution of sodium octylsulfonate (5−10-fold excess relative to Br^-; renewed frequently) at ambient temperature for several days, followed by dialysis against pure water to eliminate excess surfactant and NaBr microions. The contents of the dialysis bag were then freeze-dried, followed by further drying in vacuo for at least 2 days at 60 °C before chemical analysis. The procedure was repeated, as necessary, until EDX indicated no remaining Na or Br ions.

Elemental analysis, and in particular the S/N ratios, confirmed the completeness of ion exchange and indicated also the satisfactory purity of the complexes. Furthermore, the ratio of the integrated NMR signals corresponding to the two components indicated that the substitution of the bromide counterions by octylsulfonate was essentially quantitative. This is shown in Figure 2 for P12DMAP*b*-S8 in D_2O by the clearly defined and isolated signals of the polymer at 8.32 and 7.17 ppm and of the surfactant at 3.01 ppm (verified also in DMSO). The thermal stability of P12DMAP-S8 was found to be greater than that of P12DMAP-Br (5% weight loss of 330 °C compared to 265 °C); the others were not tested. Greater thermal stability of alkylsulfonate-neutralized polyamphiphiles compared to Br-neutralized counterparts was also observed for the methylpyridinium series.[11]

8-Methacryloyloxyoctyl(4-dimethylamino)pyridinium Bromide (M8DMAP-Br). In the form of a white crystalline powder. ^{1}H NMR [$(CD_3)_2SO$, ambient]: $\delta = 8.32$ [d, 2H, pyridinium in α position], 7.03 [d, 2H, pyridinium in β position], 5.98 [s, 1H, C*H*═C(CH$_3$)−COO cis], 5.65 [s, 1H, C*H*═C(CH$_3$)−COO trans], 4.16 [t, 2H, CH_2−N$^+$], 4.06 [t, 2H, CH_2−O], 3.18 [s, 6H, (CH_3)$_2$−N)],

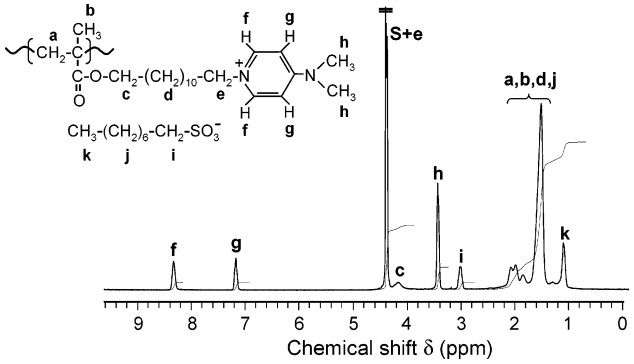

Figure 2. ^{1}H NMR spectrum of P12DMAP-S8 in D_2O (70 °C).

1.85 [s, 3H, CH═C−CH_3], 1.74 [m, 2H, CH_2−C−N$^+$], 1.58 [m, 2H, CH_2−CH$_2$−O], 1.26 [m, 8H, CH$_2$−(CH_2)$_4$−CH$_2$].

Poly(8-methacryloyloxyoctyl(4-dimethylamino)pyridinium bromide) (P8DMAP-Br). In the form of a white freeze-dried fluff. Anal. Calcd for [$C_{19}H_{31}N_2O_2Br$, 0.1 H_2O]$_n$: C, 56.89; H, 7.84; N, 6.99. Found: C, 57.01; H, 8.33; N, 6.76. ^{1}H NMR [$(CD_3)_2SO$, ambient]: δ = 8.49 [one broad signal, 2H, pyridinium in α position], 7.07 [d, 2H, pyridinium in β position], 4.25 [one signal, CH_2−N$^+$], 3.8−4.1 [CH_2−O; broad and overlapped by CH_2−N$^+$], 3.18 [s, 6H, (CH_3)$_2$−N], 1.9−0.9 [broad signals, CH_2 (backbone, spacer) and CH_3 (backbone)].

Poly(8-methacryloyloxyoctyl(4-dimethylamino)pyridinium octylsulfonate) (P8DMAP-S8). In the form of a white freeze-dried fluff. Anal. Calcd for [$C_{27}H_{48}N_2O_5S$]$_n$: C, 63.25; H, 9.44; N, 5.46; S, 6.25; S/N = 1.14. Found: C, 62.76; H, 9.78; N, 5.21; S, 6.09; S/N = 1.17. ^{1}H NMR [$(CD_3)_2SO$, ambient]: δ = 8.40 [one broad signal, 2H, pyridinium in α position], 7.04 [d, 2H, pyridinium in β position], 4.19 [one signal, CH_2−N$^+$], ∼4.1 [CH_2−O, barely visible shoulder on CH_2−N$^+$ signal], 3.16 [s, 6H, (CH_3)$_2$−N], 2.38 [t, 2H, CH_2−SO$_3^-$], 1.8−0.9 [broad signals, CH_2 (backbone, spacer) and CH_3 (backbone)], 0.81 [t, 3H, CH_3 (surfactant)].

12-Methacryloyloxydodecyl(4-dimethylamino)pyridinium Bromide (M12DMAP-Br) and Poly(12-methacryloyloxydodecyl(4-dimethylamino)pyridinium bromide) (P12DMAP-Br). See Experimental Section in ref 6.

Poly(12-methacryloyloxydodecyl(4-dimethylamino)pyridinium octylsulfonate) (P12DMAP-S8). In the form of a white freeze-dried fluff. Polymer polymerized with no transfer agent present (P12DMAP*a*-S8): Anal. Calcd for [$C_{31}H_{56}N_2O_5S$, 3 H_2O]$_n$: C, 59.77; H, 10.03; N, 4.50; S, 5.15; S/N, 1.15. Found: C, 59.41; H, 9.61; N, 5.35; S, 6.17; S/N = 1.15). Polymer polymerized in the presence of transfer agent (P12DMAP*b*-S8): Anal. Calcd for [$C_{31}H_{56}N_2O_5S$, 0.3H_2O]$_n$: C, 64.81; H, 10.18; N, 4.75; O, 15.42; S, 5.46; S/N, 1.15. Found: C, 64.61; H, 10.15; N, 4.74; O, 15.42; S, 5.40; S/N = 1.14. ^{1}H NMR (D_2O, 70 °C; Figure 2): δ = 8.32 [one signal, 2H, pyridinium in α position], 7.17 [one signal, 2H, pyridinium in β position], 4.35 [overlapped by H_2O peak, CH_2−(N$^+$)], 4.15 [broad, CH_2−O], 3.42 [broad, 6H, (CH_3)$_2$−N], 3.01 [one signal, 2H, CH_2−SO$_3^-$], 2.2−1.2 [broad, CH_2 (backbone, spacer, surfactant) and CH_3 (backbone)], 1.09 [one signal, 3H, CH_3 (surfactant)].

16-Methacryloyloxyhexadecyl(4-dimethylamino)pyridinium Bromide (M16DMAP-Br). Yield: 69% in the form of a white powder. Melting point: 94 °C (DSC peak temperature for a scan rate of 10 °C/min). Anal. Calcd for $C_{27}H_{47}N_2O_2Br$, 1.0 H_2O: C, 61.23; H, 9.33; N, 5.29; O, 9.06; Br, 15.09. Found: C, 61.48; H, 9.44; N, 4.89; O, 9.32; Br, 14.87. ^{1}H NMR ($CDCl_3$, ambient): δ = 8.27 [d, 2H, pyridinium in α position], 6.99 [d, 2H, pyridinium in β position], 6.08 [s, 1H, CH═C(CH$_3$)−COO cis], 5.56 [s, 1H, CH═C(CH$_3$)−COO trans], 4.28 [t, 2H, CH_2−N$^+$], 4.15 [t, 2H, CH_2−O], 3.30 [s, 6H, (CH_3)$_2$−N)], 1.95 [s, 3H, CH═C−CH_3], 1.91 [m, 2H, CH_2−C−N$^+$], 1.67 [m, 2H, CH_2−CH$_2$−O], 1.45−1.10 [m, 28H, CH$_2$−(CH_2)$_{14}$−CH$_2$].

Poly(16-methacryloyloxyhexadecyl(4-dimethylamino)pyridinium bromide) (P16DMAP-Br). In the form of a white freeze-dried fluff. Anal. Calcd for [$C_{27}H_{47}N_2O_2Br$, 1 H_2O]$_n$: C, 61.23; H, 9.33; N, 5.29. Found: C, 61.73; H, 9.71; N, 5.08. ^{1}H NMR (D_2O, ambient): δ = 8.72 [one broad signal, 2H, pyridinium in α position], 7.52 [d, 2H, pyridinium in β position], 4.75 [one signal, overlapped by the H_2O signal at 4.80, CH_2−N$^+$], 4.52 [broad, CH_2−O], 3.75 [s, 6H, (CH_3)$_2$−N], 2.8−1.2 [broad signals, CH_2 (backbone, spacer) and CH_3 (backbone)].

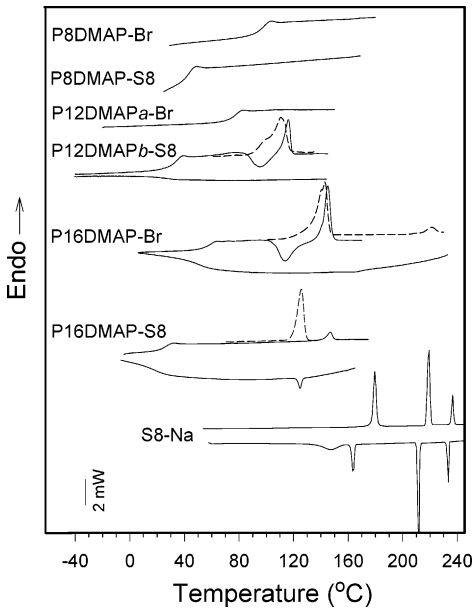

Figure 3. DSC thermograms of the polyamphiphiles (PnDMAP-Br) and polyamphiphile−octylsulfonate complexes (PnDMAP-S8), scanned at 20 °C/min, and of octylsulfonate (S8-Na) scanned at 10 °C/min.

Table 1. DSC Data for the Polyamphiphiles (PnDMAP-Br) and the Polyamphiphile−Surfactant Complexes (PnDMAP-S8)[a]

polymer	T_g[b] (°C)	T_M[c] (°C)	ΔH_M[c] (J/g)	T_I (°C)	ΔH_I (J/g)
P8DMAP-Br	97				
P8DMAP-S8	43				
P12DMAP-Br	76				
P12DMAP-S8	35	115[d]	12		
P16DMAP-Br	60	145	15	222[c]	1.1[c]
P16DMAP-S8	29	126	15	149	1.5

[a] T_g, glass transition temperature; T_M and ΔH_M, melting point and enthalpy; T_I and ΔH_I, clearing point and enthalpy. [b] The heat capacity change of all of the T_g's is about 0.3 J g^{-1} K^{-1}. [c] Measured on the first scan. [d] For P12DMAP*b*-S8 only (5−10 °C lower for P12DMAP*a*-S8; sample dried at about 90 °C to avoid melted form).

Poly(16-methacryloyloxyhexadecyl(4-dimethylamino)pyridinium octylsulfonate) (P16DMAP-S8). In the form of a white freeze-dried fluff. Anal. Calcd for [$C_{35}H_{64}N_2O_5S$, 1.0 H_2O]$_n$: C, 65.28; H, 10.48; N, 4.35; O, 14.91; S, 4.98; S/N, 1.14. Found: C, 65.74; H, 10.40; N, 4.28; O, 14.69; S, 4.74; Br, 0.15; S/N = 1.11. ^{1}H NMR [$(CD_3)_2SO$, ambient]: δ = 8.40 [d, pyridinium in α position], 7.04 [d, pyridinium in β position], 4.18 [t, CH_2−N$^+$]; 4.0−3.7 [broad, one signal, broad and overlapped by CH_2−N$^+$; CH_2−O], 3.17 [s (CH_3)$_2$−N], 2.39 [t, CH_2−SO$_3^-$], 1.8−1.0 [CH_2 (backbone, spacer, surfactant) and CH_3 (backbone)], 0.83 [t (indistinct), CH_3 (surfactant)].

Results and Discussion

PnDMAP-Br Polyamphiphiles. Representative DSC thermograms of the three Br-neutralized polyamphiphiles are shown in Figure 3, and the values associated with the various transitions are given in Table 1. The ambient-temperature X-ray diffractograms of the polyamphiphiles are shown in Figure 4, with associated values given in Table 2.

P8DMAP-Br and P12DMAP-Br display simple thermograms, with a well-defined glass transition (T_g) only and no first-order

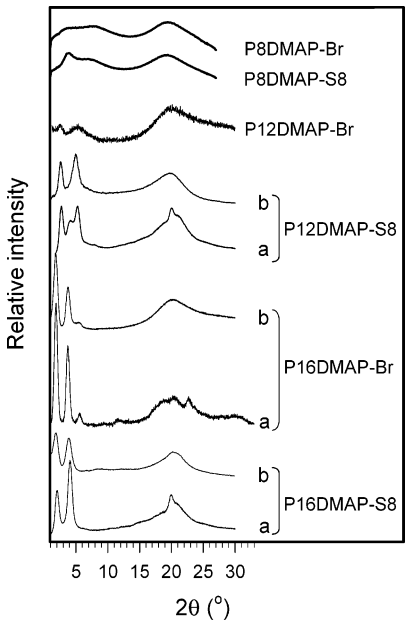

Figure 4. Ambient temperature X-ray diffractograms of the polyamphiphiles, PnDMAP-Br, and the polyamphiphile−octylsulfonate complexes, PnDMAP-S8: (a) as-prepared (or annealed) samples; (b) previously melted samples.

peaks, as observed previously for other tail-end pyridinium polyamphiphiles.[6] The X-ray diffractogram of P12DMAP-Br (Figure 4, curve c) suggests that it tends to organize as a disordered lamellar (smectic A-like) superstructure, in accordance with which it shows weak birefringence between crossed polarizers. The diffractogram of P8DMAP-Br (Figure 4, curve a) shows only a hint of the same tendency and even weaker birefringence between crossed polarizers. The birefringence decreases gradually with temperature to finally disappear, which can be rationalized by a progressive decrease in the sizes of the ordered domains to below the wavelength of visible light.[6,11,17]

The longer-spacer polyamphiphile, P16DMAP-Br, is characterized by more complex behavior, displaying first-order transitions in addition to a T_g. It is noteworthy that the T_g's of the three polymers decrease with increasing spacer length, in accordance with the internal plasticization effect. The rate of decrease is about 5 °C per CH_2 in the spacer, which is similar to what was observed for the analogous methylpyridinium polyamphiphiles having the same spacer lengths.[6]

Regarding the first-order transitions in P16DMAP-Br, there is a relatively strong endotherm near 145 °C and a weak one that appears on first heating at 222 °C. The sample is birefringent between crossed polarizers in the temperature range between the two transitions and becomes isotropic at the higher temperature transition. It thus appears to display typical thermotropic behavior of a liquid crystalline material, with transitions from an ordered phase to a disordered liquid crystal mesophase to the isotropic phase. On cooling, a very weak transition appears near 170 °C. This is considerably lower in temperature than the clearing point (particularly in comparison to corresponding data for P16DMAP-S8; see below), which is probably caused, at least partly, by some degradation having occurred at high temperature (as supported by the irreproducibility of this transition in subsequent scans) and possibly also by a kinetic effect related to the ionic interactions coupled with the polymeric character of the material. A transition back to the more ordered phase is not observed in the cooling thermograms, including in those obtained after heating scans that were limited to lower temperatures such as 160 °C. However, an exothermic dip near 115 °C, indicating recrystallization, consistently occurs in subsequent heating thermograms for samples not subjected to high (isotropization) temperatures.

The ambient temperature X-ray diffractograms of P16DMAP-Br before and after melting are compared in Figure 4. The various weak and broad reflections superposed on a diffuse halo in the wide-angle region for the unmelted sample are indicative of a low degree of crystallinity (consistent with the moderate enthalpy values of the melting and recrystallization transitions in DSC). Following melting, the cooled sample shows no evidence of crystallinity in the diffractograms, in accordance with the DSC data, whereas annealing at temperatures in the region of the DSC recrystallization exotherm regenerates the initial profile.

In the low-angle region, three sharp reflections of decreasing intensity and with reciprocal spacings in the ratio 1:2:3 are apparent for both the partially crystalline sample and for the previously melted noncrystalline sample. The presence of three diffraction orders is another unique feature of P16DMAP-Br compared to the other polyamphiphiles we studied, which all show two diffraction orders in the ratio 1:2. It provides clear evidence that the supramolecular organization of the liquid crystal phase is lamellar in character, specifically smectic A (or C). The sharpness of the reflections indicates a longer correlation length of the lamellar order for P16DMAP-Br compared to P12DMAP-Br and P8DMAP-Br. The increase in correlation length with increase in spacer length was also observed for the methylpyridinium series, but the difference between $n = 12$ and 16 was less pronounced than in the present case.[6] In fact, P12DMAP-Br was observed to be the least organized of the 12-carbon spacer polyamphiphiles that we investigated, which was attributed to its greater bulkiness. The present result suggests that, due most likely to this bulkiness, greater decoupling from the main chain is required in order for the DMAP moieties to pack efficiently; this appears to be achieved between 12 and 16 methylene units in the spacer.

The lamellar spacings, d_B, determined from the X-ray data for the three polyamphiphiles are given in Table 2. Although d_B increases with increase in spacer length, as expected, it is noted that when they are compared with the calculated molecular lengths of the polymer repeat unit, l_M, the ratio d_B/l_M increases from 1.0 for $n = 8$ to 1.4 for $n = 16$. This parallels what was observed for the methylpyridinium series.[6] Assuming a smectic A rather than C phase (as indicated by an X-ray diffractogram of an oriented polyamphiphile[11]), it suggests that the packing structure evolves from an effective monolayer arrangement to a partial bilayer arrangement (i.e., a bilayer with partial overlap or interdigitation of the side chains[18]) with increase in spacer length. In this case, the liquid crystal phase in P16DMAP-Br can be identified as a partial bilayer smectic A mesophase. The fact that the lamellar spacing is somewhat smaller at higher temperatures (see Table 2 for the data at 160 °C), as is usual for smectic A mesophases, supports this assignment. It is noted also that there is no significant difference in the lamellar spacing whether or not crystallinity is present. Of all the (Br-neutralized) pyridinium-based tail-end polyamphiphiles studied by us, including the 16-spacer methylpyridinium polymer mentioned above,[6] P16DMAP-Br is the only one found to possess some crystalline order. Furthermore, it contrasts with the methylpyridinium analogue, which, in addition, shows no isotropization temperature but instead maintains its disordered lamellar state until degradation temperatures[6] indicative of greater thermal stability for this phase.

Table 2. Bragg Spacings, d_B (First/Second/Third Reflections), Obtained from the X-ray Diffraction Data in the Small-Angle Region and Calculated Molecular Lengths, l_M, of the Side-Chain Repeat Unit, for the Polyamphiphiles and Their Complexes

	d_B (Å)				
polymer	RT[a]	RT[b]	high T	l_M (Å)	d_B/l_M (RT)
P8DMAP-Br	23/11			23.3	1.0
P8DMAP-S8	23/12			*f*	
P12DMAP-Br	35/17			28.4	1.2
P12DMAP-S8	33.9/17.4	35.0/17.8	32.6/16.6[c]	*f*	
P16DMAP-Br	47.5/23.6/15.8	47.7/23.5/16	37.4/19.2[d]	33.4	1.4
P16DMAP-S8	43.3/21.7	46.0/22.8	38.8/19.4[e]	*f*	

[a] Ambient temperature after drying or annealing (P12DMAP-S8, P16DMAP-Br, and P16DMAP-S8 are partially crystalline). [b] After cooling from the melt to ambient temperature; noncrystalline. [c] At 90 °C. [d] At 160 °C. [e] At 135 °C. [f] The calculated molecular length for the S8 counterion is 9.3 Å.

PnDMAP-S8 Complexes: Thermal Behavior. The DSC thermograms of the PnDMAP-S8 complexes, and associated values, are compared with the parent Br polyamphiphiles in Figure 3 and Table 1, respectively. The pure Na-neutralized surfactant (scanned at 10 °C/min) is also shown in Figure 3 and is clearly characterized by a rich thermotropism up to high temperatures.[19] In the complexes, a well-defined T_g remains present and is depressed in temperature compared to the Br-neutralized homologues, which is attributed to the additional plasticizing effect of the alkyl chain of the surfactant. The rate of T_g decrease with increase in spacer length in these complexes is about 2 °C/CH_2, much lower than that observed for the Br analogues. This may reflect a reduction in plasticizing efficiency of the side chains when they exceed an optimal length.

No additional transitions are observed by DSC for P8DMAP-S8, and the birefringence between crossed polarizers is similar to that observed for its Br-neutralized counterpart. The two longer spacer complexes, P12DMAP-S8 and P16DMAP-S8, display a relatively intense first-order transition in the first DSC heating scan, indicating the presence of an ordered or crystalline phase (confirmed by X-ray diffraction; see later), with no crystallization occurring during the cooling scans. For P12DMAP*b*-S8 (polymer synthesized in the presence of transfer agent), shown in Figure 3, this transition is also present in subsequent scans following a recrystallization exotherm (or after annealing near 90 °C), as observed for P16DMAP-Br. For P12DMAP*a*-S8 (polymer synthesized without transfer agent present), recrystallization is not observed in subsequent heating scans, and only a glass transition is visible; instead, long annealing times are required to obtain crystallization; e.g., a broad peak centered at about 105 °C with an enthalpy of about 6 J/g is observed after annealing the previously scanned DSC sample in a vacuum oven at about 75 °C for 4 days. This can be rationalized by the presumably greater molecular weight of the latter polymer, with a resulting increase in the melt viscosity, which may further slow down the already sluggish crystallization rate. Between crossed polarizers, P12DMAP-S8 shows no birefringence above the melting point (in contrast to P16DMAP-Br).

P16DMAP-S8, on the other hand, displays two first-order transitions, which correspond to transitions from an ordered phase to a liquid crystal mesophase to isotropization (see later for the X-ray data), like its Br-neutralized counterpart. The melting point occurs at a somewhat lower temperature for the complex compared to P16DMAP-Br (by about 15 °C), whereas the clearing point is greatly reduced by the surfactant (by more than 70 °C). Thus, the surfactant has a strong destabilizing effect on the mesophase, but much less on the more ordered phase. The isotropic to liquid crystal transition is also clearly apparent in the cooling thermograms, with a supercooling of about 25 °C. This supercooling, which is greater than generally observed for LC−isotropic transitions in side-chain LCP's analyzed in the same conditions,[20] indicates a kinetic effect on the transition, probably due, at least in part, to the high viscosity resulting from the ionic interactions and polymeric character, as suggested above for P16DMAP-Br.

In subsequent heating scans, no recrystallization occurs, and even after long annealing times there is little or no crystallization (for example, no evidence of crystallinity was observed after 1 week of annealing at about 75−80 °C, whereas a very low-intensity DSC melting peak ($\Delta H \sim 0.6$ J/g) at 125 °C was obtained after annealing for 2 days at 100 °C). Evidently, the longer alkyl chain of the surfactant, despite its plasticizing effect on the T_g of this complex, does not facilitate crystallization. Possibly, this is related, in addition to the ionic and polymer factors mentioned above, to increased interactions (or miscibility) between the alkyl chain of the surfactant and the much longer alkyl spacer of the polyamphiphile that may add to the difficulty of reorganization into a more ordered structure required for crystallization (this may also account for, or contribute to, the destabilizing effect of the surfactant on the mesophase compared to P16DMAP-Br). In addition, the two different resonance structures of DMAP (Figure 1), which can allow complexation at two different sites and thus influence the location of the surfactant counterion, may play a role in obstructing crystallization from the melt. The repression of crystallization in this complex has the effect that the liquid crystal structure is stable indefinitely at and above ambient temperature, which is attractive for applications where crystallinity is undesired.

PnDMAP-S8 Complexes: Structural Properties. Ambient temperature X-ray diffractograms of the complexes are shown in Figure 4, and the associated data are given in Table 2. The diffractogram for P8DMAP-S8 is similar to that of its Br counterpart, except for a somewhat better defined small-angle reflection corresponding to a Bragg spacing of about 23 Å. With increasing temperature, the intensity of this reflection gradually decreases and moves to slightly larger angles (corresponding to 21 Å at 140 °C). This behavior is very similar to that of P12DMAP-Br and other Br-neutralized polyamphiphiles, as described and rationalized above.

The diffractogram of P12DMAP-S8 before melting shows a wide-angle reflection at 20° (4.4 Å) superimposed on an amorphous halo, indicative of a low degree of crystallinity. The asymmetry of the halo suggests the presence of another peak, shown in Figure 5 to be broad and centered at about 21.5° (4.1 Å). These peaks are most likely related to crystallization at the tail-end of the surfactant,[11] as will be further commented on later. When melted and cooled back to room temperature, only an amorphous halo is observed at wide angles. There are also two approximately equidistant reflections in the low-angle region, suggestive of smectic liquid crystal order. As shown in Figure 6 for the previously melted P12DMAP*a*-S8 complex (maintained in a vacuum oven at about 100−110 °C for 2 days just before analysis), these reflections remain very apparent on

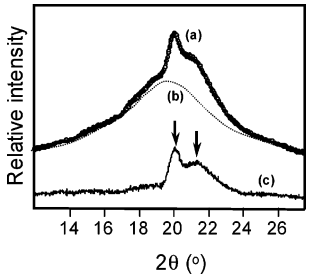

Figure 5. Ambient temperature X-ray diffractogram of the P12DMAP*b*-S8 complex in the wide-angle region, illustrating the presence of two reflections after subtraction of the amorphous halo.

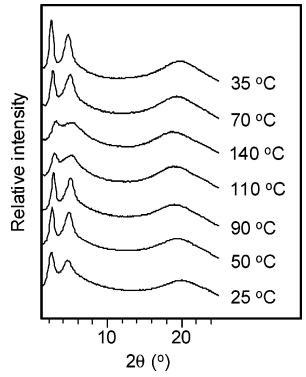

Figure 6. X-ray diffractograms of the previously melted P12DMAP*a*-S8 complex at the nominal temperatures indicated, taken in order from bottom to top.

heating until at least 90 °C (and move to slightly smaller Bragg spacings) but are very weak by 110 °C, and they reappear on cooling. This illustrates that the complex is mesomorphic up to a fairly well-defined temperature zone, despite the absence of a LC−isotropic transition in the DSC curves (in particular, for P12DMAP*a*-S8 for which heating thermograms without recrystallization were obtained; see above). This temperature zone is in the same region as the melting peak and is thus consistent with the fact that the complex appears isotropic between crossed polarizers above the melting point. It can be compared with the observation that the Br-neutralized counterpart gradually loses its birefringence in the range between its T_g and 100 °C, with no DSC transition apparent.[6]

In the partly crystallized sample, the small-angle region shows the same two equidistant reflections at about the same positions as in the noncrystalline sample. In addition, there are two other very weak reflections that appear approximately equidistant and that, when taken as first- and second-order reflections, correspond to a Bragg spacing of about 22 Å, which is smaller than the P12DMAP side chain length (ca. 28 Å, not including the surfactant) and a little more than twice the surfactant length (ca. 19 Å). These were observed for both of the P12DMAP-S8 complexes (checked, in particular, using the annealing conditions mentioned above for the DSC experiment). It is thus concluded that these two weak reflections are related to the crystalline structure that coexists with the noncrystalline structure.

The P16DMAP-S8 complex shows the same characteristics as P12DMAP-S8 in the wide-angle region: namely, a diffuse halo for the previously melted sample and a weak reflection at 4.4 Å as well as the suggestion of another at 4.1 Å superposed on the diffuse halo for the partly crystalline sample. In the small-angle region, however, there is no evidence of additional peaks in the partly crystalline sample other than the two equidistant reflections present for the previously melted sample (possibly because they are coincident for the crystalline and noncrystalline

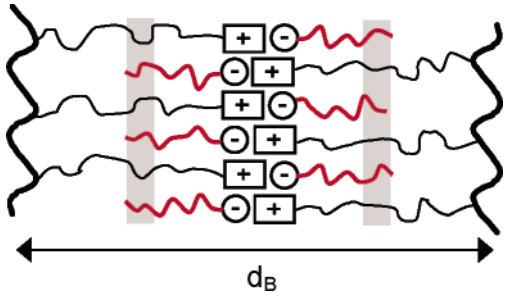

Figure 7. Simplified schematic of a possible packing model for the PnDMAP-S8 complexes. The gray bars indicate regions of potential crystallization (see text).

structures). The only differences in this region between the unmelted and previously melted samples are the greater intensity and narrowness of the reflections for the partly crystalline sample. It is also noted that the Bragg spacing of the complex decreases with temperature as for P16DMAP-Br, again consistent with smectic A behavior.

In the isotropic region of P12DMAP-S8 (see Figure 6) and P12DMAP-S16, the two small-angle peaks are drastically decreased in intensity, although still present (as was observed also for P12MP-S8[11]): this may indicate a tendency to maintain the same order over a short correlation length or it may be related to a "correlation hole" effect.[21,22] The pattern is not so different from what is observed for $n = 8$ (Br- and S8-neutralized), although the latter shows slight birefringence between crossed polarizers.

Whereas the X-ray diffractograms clearly show that the liquid crystal or mesomorphic phase is reversible with temperature for both P12DMAP-S8 and P16DMAP-S8, these samples show little birefringence between crossed polarizers when cooled from the isotropic state. This may be due to a tendency to homeotropic orientation assuming smectic A order (but shearing of the sample does not provoke increased birefringence), to mesomorphic domains that remain smaller than the wavelength of light (which, if true, might be attributed to slow growth from many points due to the high viscosity of these materials), or to the absorption of H_2O during the POM observations that in some of the polyamphiphiles investigated appears to give rise to cubic phases (which are not birefringent).[11,23]

It is striking that the ambient temperature Bragg spacings of the complexes are essentially the same as their Br counterparts. In other words, the replacement of Br by the much longer S8 counterion does not change the fundamental period of the packing structure. Only the spacer length of the polyamphiphile seems to be determinant. This was observed also for the 12-carbon spacer methylpyridinium (MP) polyamphiphile with the same surfactant counterion (S8) and with shorter (S4) and longer (S16) surfactant counterions.[11] In the present case, it seems reasonable to postulate that the surfactant, S8, whose alkyl chain is equal to or shorter than the alkyl spacer in the PnDMAP series, is packed in the same plane as the alkyl spacers, as shown by the schematic model given in Figure 7. This model is also appealing with regard to optimized ionic interactions, especially in view of the possible resonance structures of the DMAP moiety (see Figure 1). The basic model, that is, with removal of the red lines (representing the surfactant alkyl chains) and with greater lateral disorder drawn for the black lines (representing the spacer), was originally proposed[6] as a possible molecular packing arrangement for the various bromine-neutralized pyridinium polyamphiphiles studied, which can account for the experimental lamellar thicknesses that suggest partial bilayer

packing for 12- and 16-methylene spacers, as here for PnDMAP-Br.

However, a number of experimental details are not easily rationalized by this model or require additional arguments. First, considering only the Br-neutralized polyamphiphiles, it is unclear how to explain the increase in Bragg spacing relative to the calculated molecular length (d_B/l_M ratio) with increase in spacer length from 8 to 16. Second, the replacement of Br by S8 counterions would be expected to reduce the lateral disorder of the alkyl spacer (at least the eight or so methylene units nearest the pyridinium group) in order to accommodate the alkyl chains of S8 and thus should result in an increase in the Bragg spacing (for a given spacer length), which is not observed. Third, it is difficult to rationalize surfactant tail-end crystallization by this model. It could be postulated that, for the 12- and 16-methylene spacer lengths, the surfactant tail ends might crystallize along with the adjacent methylene groups of the spacer as shown by the gray bars in Figure 7; however, the proximity of the backbone, especially for $n = 12$, does not favor this possibility. Clearly, further investigations are necessary to clarify the packing arrangement. It may be mentioned that another, more complex packing model, where the surfactant alkyl chains are segregated from the alkyl spacers, was proposed in ref 11, but since the present data do not lend additional support (nor give clear contradictory evidence) for this model, it will not be discussed here.

Concluding Remarks and Overview

The series of polyamphiphiles investigated in this contribution illustrates that the thermal and mesomorphic behavior of the system can be manipulated by the spacer length and choice of counterion. In parallel with the methylpyridinium (MP) bromide series,[6] it is observed that a spacer length of eight methylene units is near the lower limit of the range where (lamellar) mesomorphic self-assembly is possible in this family of materials. Increase of the spacer length to 12 improves the lamellar order, but it remains weak for DMAP compared to other pyridinium polyamphiphiles; this is attributed to the greater bulkiness of the dimethylamino extremity in the former, which apparently necessitates greater decoupling from the polymer backbone to allow well-defined organization. At this spacer length, no definite clearing point to an isotropic phase is observed, although birefringence between crossed polarizers gradually disappears at higher temperatures, rationalized by slowly decreasing mesomorphic domain sizes to below the wavelength of light as temperature is increased.[6] A spacer length of 16, however, results in a well-behaved thermotropic material with both a crystalline phase and a smectic A-like phase with a high correlation length and a well-defined clearing point at high temperature (>200 °C). In contrast, the only other polyamphiphile with a 16-methylene spacer studied, MP, shows no crystallinity, and its smectic A-like phase remains stable up to degradation temperatures.[6] The glass transition decreases at a similar rate with increase in spacer length in the DMAP and MP series.

Ion exchange of the Br counterion by octylsulfonate has little effect on the shortest spacer polyamphiphile other than decreasing its glass transition considerably and improving the structural organization slightly. For the spacer length of 12, however, the octylsulfonate counterion induces a crystalline phase in the DMAP polyamphiphile. This contrasts with the analogous MP polyamphiphile, which shows only glass transition phenomena; in fact, two T_g's (or T_g-like transitions) were detected by DSC for both butyl- and octylsulfonate counterions[11] (a second T_g-like transition is possibly present as well in noncrystallized P12DMAP-S8, in the 60−70 °C region; see Figure 3). In both systems, disordered lamellar (smectic A) organization is clearly evidenced by XRD and reversibly enters an isotropic state, but no corresponding transition is detectable by DSC (like for the Br-neutralized forms). XRD indicates that isotropization is reached in the vicinity of the melting point for P12DMAP-S8. On the other hand, the pyridylpyridinium (PP) analogue, neutralized by Br- and to which octylphenol is associated by hydrogen bonding to the pyridyl end group, also displays a crystalline and a smectic A phase (not observed in the absence of octyl phenol), this time with a well-defined clearing point in DSC.[12] Interestingly, the melting points of the crystalline phases in the DMAP and PP complexes are essentially the same (115 °C). Similar overall behavior is observed when other (azo-containing) phenol derivatives are added to the PP polyamphiphile.[24]

P16DMAP-Br is the only 16-spacer tail-end pyridinium polyamphiphile to have been ion-exchanged by a surfactant counterion to date. By comparison to the Br-neutralized analogue, the thermal stability of the already present crystalline and smectic A phases in P16DMAP-S8 is affected: the crystalline phase melts at a somewhat lower temperature (∼20 °C lower), and the liquid crystal phase reaches isotropization at a much lower temperature (∼75 °C lower). The destabilization of the liquid crystal phase may be caused by the flexible alkyl chain of the surfactant and/or by the change in anion (change in size and/or ionic strength). On the other hand, by comparison to P12DMAP-S8, the 16-spacer complex has higher melting and clearing points, translating the effect of increased decoupling of the pyridinium group from the polymer backbone that enhances the formation and stability of both the crystal and liquid crystal phases. It may be added, in this connection, that the previously studied P12MP series[11] showed that increasing the surfactant length has a similar effect; that is, both a reversible crystalline and a well-defined liquid crystalline phase are obtained for P12MP-S16 (not observed for P12MP-S8, as mentioned above), with a melting point in the same range as that for P12DMAP-S8 and a clearing point that is nearly 20 °C higher than for P16DMAP-S8. From these data, it might be guessed that replacement of S8 by S16 in P16DMAP should lead to enhanced stability of the ordered phases.

The crystallinity that is observed in these materials is always partial (as shown by the superposition of one or more reflections on a wide-angle halo in the X-ray diffractograms) and might be ascribed to the tail ends only, as is observed for many comblike polymers, in particular long aliphatic side-chain polymers,[25,26] polyelectrolyte−surfactant complexes,[27,28] and the polyamphiphile complexes already mentioned.[11,12] Crystallization involving alkyl chains typically gives rise to one or two wide-angle X-ray reflections in the 20°−25° (2θ) range depending on the nature of the alkyl chain packing (generally hexagonal or orthorhombic; see ref 11 and references therein for a more detailed discussion). The wide-angle X-ray pattern of the crystalline phase is identical for the two S8-neutralized DMAP polyamphiphiles and consistent with alkyl chain crystallization.

Once melted, all of the initially crystalline DMAP-based materials studied here recrystallize with difficulty, as shown by the absence of crystallization in the DSC cooling thermograms (for P16DMAP-S8 and P12DMAP*a*-S8, no crystallization occurs in subsequent heating thermograms either; instead, long annealing times are needed to induce crystallization, still particularly difficult for P16DMAP-S8). This is probably related to the presence of the ionic groups, coupled with the polymeric

character of the materials, both of which decrease mobility and hence increase the viscosity in the melt.[29] As discussed above, different resonance structures of DMAP (allowing complexation of the surfactant counterion at different locations) and easy mixing of the alkyl chains of the surfactant with the much longer alkyl spacers of the polyamphiphile may also play a role. The absence of crystallization can be an advantage when noncrystalline but ordered structure, as in anisotropic glasses, is desired for particular applications. In contrast, crystallization occurs easily in P12MP-S16,[11] which might be attributed to the melt mobility (or plasticization) of the longer surfactant alkyl chain that, moreover, may be too long to mix easily with the polyamphiphile spacer. Complexes based on P12PP, where octylphenol[12] or other phenol derivatives with alkyl tails[24] are hydrogen-bonded to the pyridyl extremity, also tend to crystallize easily. This may be rationalized by the thermal lability of the hydrogen bond, which presumably enhances mobility in the system at higher temperatures. On the other hand, the presence of a polar tail in the phenol derivatives strongly hampers recrystallization, probably due to dipolar interactions between the polar tails and the ionic groups of the complexes in the melt.[24]

The combination of ionic interactions and polymeric character is probably largely responsible as well for the ill-defined mesomorphic−isotropic transition (i.e., the absence of a DSC signal) in the polyamphiphiles for which there is not a compensating factor. This has been observed in almost all of the Br-neutralized polyamphiphiles studied to date (except for P16DMAP-Br of the present study), as well as in most complexes with 12 or less carbon spacers and sulfonate counterions of 8 or less carbons in the alkyl chain. On the other hand, increasing either the spacer length or the counterion chain length to 16 carbons allows sufficient mobility and/or long-range ordering to result in more classic thermotropic behavior (with well-defined DSC transitions). In the P12PP-based system, a surfactant chain of eight carbons is sufficient to result in the same behavior,[12] which can be related to the mobility of the H-bond. H-bond mobility appears to allow typical thermotropic expression in P12PP-based complexes even for shorter, more rigid phenol derivatives; however, the presence of a polar (cyano) tail in the phenol derivative was observed to retard the development of the LC phase from the isotropic state, attributed again to dipolar interactions between this tail and the ionic groups.[24]

Finally, the present study confirms the tendency observed for the other pyridinium-based materials that have been investigated concerning the Bragg distance (lamellar thickness), d_B. Notably, d_B depends primarily on the spacer length of the polyamphiphile and very little if at all on the counterion be it simple bromine or an alkyl surfactant of variable alkyl chain lengths (it does appear to be modified, however, by rigid-rod-like molecules complexed to the end of the side chains[24]). This indicates that the surfactant chain is somehow accommodated within the same molecular packing structure as the Br-neutralized parent polyamphiphiles.

Acknowledgment. The financial support of NSERC (Canada) and FQRNT, formerly FCAR (Québec), is gratefully acknowledged. We thank Dr. J.-C. Galin of Institut Charles Sadron (ICS), Strasbourg, France, for overseeing the elemental analyses performed at ICS and Dr. M.-R. van Calsteren of Food Research and Development Center (Agriculture and Agri-food Canada, St-Hyacinthe (QC)) for some of the NMR spectra. P.Y.V. and C.G.B. acknowledge their past membership in the FCAR-funded Centre de recherche en sciences et ingénierie des macromolécules (CERSIM, Université Laval). X.S. and C.G.B. acknowledge their current membership in the FQRNT-funded, multi-university Centre for Self-Assembled Chemical Structures (CSACS).

References and Notes

(1) Rullens, F.; Vuillaume, P. Y.; Moussa, A.; Habib-Jiwan, J.-L.; Laschewsky, A. *Chem. Mater.* **2006**, *18*, 3078.
(2) Vuillaume, P. Y.; Glinel, K.; Jonas, A. M.; Laschewsky, A. *Chem. Mater.* **2003**, *15*, 3625.
(3) Laschewsky, A. *Adv. Polym. Sci.* **1995**, *124*, 1.
(4) Binnemans, K. *Chem. Rev.* **2005**, *105*, 4148.
(5) Masson, P.; Guillon, D. *Mol. Cryst. Liq. Cryst.* **2001**, *362*, 313.
(6) Vuillaume, P. Y.; Bazuin, C. G.; Galin, J. C. *Macromolecules* **2000**, *33*, 781.
(7) Koberle, P.; Laschewsky, A. *Macromolecules* **1994**, *27*, 2165.
(8) Laschewsky, A.; Zerbe, I. *Polymer* **1991**, *32*, 2070.
(9) Koberle, P.; Laschewsky, A.; Tsukruk, V. *Macromol. Chem. Phys.* **1992**, *193*, 1815.
(10) Tsukruk, V.; Mischenko, N.; Koberle, P.; Laschewsky, A. *Macromol. Chem. Phys.* **1992**, *193*, 1829.
(11) Vuillaume, P. Y.; Bazuin, C. G. *Macromolecules* **2003**, *36*, 6378.
(12) Bazuin, C. G.; Brodin, C. *Macromolecules* **2004**, *37*, 9366.
(13) Vuillaume, P. Y.; Galin, J. C.; Bazuin, C. G. *Macromolecules* **2001**, *34*, 859.
(14) Vuillaume, P. Y. et al. To be submitted for publication.
(15) Gottlieb, H. E.; Kotlyar, V.; Nudelman, A. *J. Org. Chem.* **1997**, *62*, 7512.
(16) Brodin, C. Ph.D. Thesis, Département de chimie, Université Laval, Québec, Canada, 2003.
(17) Ponomarenko, E. A.; Waddon, A. J.; Bakeev, K. N.; Tirrell, D. A.; MacKnight, W. J. *Macromolecules* **1996**, *29*, 4340.
(18) Barón, M. *Pure Appl. Chem.* **2001**, *73*, 845.
(19) X-ray diffractograms suggest a smectic B phase between 219 and 237 °C and a smectic A phase above 237 °C.
(20) See, for example: Ruan, J.-J.; Jin, S.; Ge, J. J.; Jeong, K.-U.; Graham, M. J.; Zhang, D.; Harris, F. W.; Lotz, B.; Cheng, S. Z. D. *Polymer* **2006**, *47*, 4182.
(21) Lipatov, Y. S.; Shilov, V. V.; Tsukruk, V. V. *Macromolecules* **1986**, *19*, 1308.
(22) Ruokolainen, J.; Torkkeli, M.; Serimaa, R.; Komanschek, B. E.; Ikkala, O.; ten Brinke, G. *Phys. Rev. E* **1996**, *54*, 6646. Huh, J.; Ikkala, O.; ten Brinke, G. *Macromolecules* **1997**, *30*, 1828.
(23) Vuillaume, P. Y. Ph.D. Thesis, Département de chimie, Université Laval, Québec, Canada, 2000.
(24) Sallenave, X.; Bazuin, C. G. Submitted for publication.
(25) Platé, N. A.; Shibaev, V. P. *J. Polym. Sci., Macromol. Rev.* **1974**, *8*, 117.
(26) (a) Lee, J. L.; Pearce, E. M.; Kwei, T. K. *Macromol. Chem. Phys.* **1998**, *199*, 1003. (b) Watanabe, J.; Ono, H.; Uematsu, I.; Abe, A. *Macromolecules* **1985**, *18*, 2141.
(27) (a) Thünemann, A. F.; Müller, M.; Dautzenberg, H.; Joanny, J. F. O.; Lowne, H. *Adv. Polym. Sci.* **2004**, *166*, 113. (b) Antonietti, M.; Burger, C.; Thünemann, A. *Trends Polym. Sci.* **1997**, *5*, 262.
(28) (a) Ponomarenko, E. A.; Waddon, A. J.; Tirrell, D. A.; MacKnight, W. J. *Langmuir* **1996**, *12*, 2169. (b) Luyten, M. C.; Alberda van Ekenstein, G. O. R.; ten Brinke, G.; Ruokolainen, J.; Ikkala, O.; Torkkeli, M.; Serimaa, R. *Macromolecules* **1999**, *32*, 4404. (c) Cai, Y.; Wang, D.; Hu, X.; Xu, Y.; Zhao, Y.; Wu, J.; Xu, D. *Macromol. Chem. Phys.* **2001**, *202*, 2434.
(29) Orler, E. B.; Moore, R. B. *Macromolecules* **1994**, *27*, 4774.

MA061477J